

# Global Biogeochemical Cycles®

## RESEARCH ARTICLE

10.1029/2024GB008359

### Key Points:

- Glacier organic and black carbon isotopes indicate spatial variation in the dominance of deposition from modern and anthropogenic sources
- Isotopic mass-balance shows that a substantial portion of organic carbon in glacier outflows is from anthropogenic aerosols (12%–91%)
- Greater relative contributions from fossil fuels leads to aged and more aromatic organic matter exported downstream

### Supporting Information:

Supporting Information may be found in the online version of this article.

### Correspondence to:

A. D. Holt,  
adh19d@fsu.edu

### Citation:

Holt, A. D., Barton, R., Wagner, S., McKenna, A. M., Fellman, J., Hood, E., et al. (2025). Widespread black carbon deposition of varied origin exported from glaciers. *Global Biogeochemical Cycles*, 39, e2024GB008359. <https://doi.org/10.1029/2024GB008359>

Received 16 SEP 2024

Accepted 11 MAR 2025

### Author Contributions:

**Conceptualization:** Amy D. Holt, Sasha Wagner, Tom I. Battin, Robert G. M. Spencer

**Formal analysis:** Amy D. Holt

**Investigation:** Amy D. Holt, Riley Barton, Sasha Wagner, Amy M. McKenna, Jason Fellman, Hannes Peter

**Project administration:** Amy D. Holt

**Resources:** Jason Fellman, Tom I. Battin, Robert G. M. Spencer






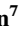



**Supervision:** Eran Hood, Robert G. M. Spencer

**Visualization:** Amy D. Holt

**Writing – original draft:** Amy D. Holt

**Writing – review & editing:** Amy D. Holt, Riley Barton, Sasha Wagner, Amy M. McKenna, Jason Fellman, Eran Hood, Tom I. Battin, Hannes Peter, Robert G. M. Spencer

## Widespread Black Carbon Deposition of Varied Origin Exported From Glaciers

Amy D. Holt<sup>1</sup> , Riley Barton<sup>2,3</sup> , Sasha Wagner<sup>2,3</sup> , Amy M. McKenna<sup>4,5</sup> , Jason Fellman<sup>6</sup> , Eran Hood<sup>6</sup> , Tom I. Battin<sup>7</sup> , Hannes Peter<sup>7</sup> , Vanishing Glaciers Field Team<sup>7,8,9</sup>, and Robert G. M. Spencer<sup>1</sup> 

<sup>1</sup>National High Magnetic Field Laboratory Geochemistry Group and Department of Earth, Ocean, and Atmospheric Science, Florida State University, Tallahassee, FL, USA, <sup>2</sup>Department of Earth and Environmental Sciences, Rensselaer Polytechnic Institute, New York, NY, USA, <sup>3</sup>Center for Environmental Stable Isotope Analysis, Rensselaer Polytechnic Institute, New York, NY, USA, <sup>4</sup>National High Magnetic Field Laboratory, Ion Cyclotron Resonance Program, Tallahassee, FL, USA, <sup>5</sup>Department of Soil Crop Sciences, Colorado State University, Fort Collins, CO, USA, <sup>6</sup>Program on the Environment and Alaska Coastal Rainforest Center, University of Alaska Southeast, Juneau, AK, USA, <sup>7</sup>River Ecosystems Laboratory, Ecole Polytechnique Fédérale de Lausanne, Lausanne, Switzerland, <sup>8</sup>Laboratorio de Limnología, Museo de Zoología QCAZ I, Escuela de Ciencias Biológicas, Pontificia Universidad Católica del Ecuador, Quito, Ecuador, <sup>9</sup>Central-Asian Institute for Applied Geosciences, Bishkek, Kyrgyzstan

**Abstract** Atmospheric deposition delivers carbon to glacier surfaces, including from fossil fuel and biomass combustion. Nonetheless, spatial variation in the sources of organic and black carbon deposited on glaciers is poorly understood, along with their role in driving glacier outflow dissolved organic matter (DOM) composition and fate. Here, we used bulk and compound-specific carbon isotopic analyses to constrain the sources of dissolved organic carbon (DOC) and dissolved black carbon (DBC) in 10 glacier outflows across four regions. To understand the relationships between glacier DOM composition and sources of DOC and DBC, isotopic data were used in conjunction with ultrahigh resolution molecular-level analyses. Globally, a substantial yet variable component of DOC was sourced from anthropogenic aerosols (12%–91%; median 50%), influencing regional DOM composition (aliphatics 26.9%–58.4% relative abundance; RA). Relatively older radiocarbon ages (i.e., larger fossil-derived component) of glacier DOC were correlated with more <sup>13</sup>C depleted DOC and DBC signatures, where DOM had higher aromaticity, elevated RA of condensed aromatics, and a lower RA of aliphatic compounds. This study highlights that anthropogenic deposition is pervasive, but its extent varies spatially with ramifications for DOM composition, and thus reactivity and fate.

**Plain Language Summary** A portion of glacier organic matter is suggested to support downstream food webs and be sourced from fossil fuel combustion byproducts. Here, glaciers across Alaska, Switzerland, Kyrgyzstan and Ecuador were analyzed using complimentary analytical techniques to determine whether glacier dissolved organic matter and combustion products (i.e., black carbon) were ubiquitously sourced from human activity. Our results highlight global variability in the contribution of fossil fuel-derived atmospheric deposition to glacier organic matter composition, with regional differences in the sources of organic and black carbon. We highlight that spatial variability in the deposition of anthropogenic fossil fuel combustion byproducts to glacier ecosystems affects both the age and character of dissolved organic matter, likely influencing its fate.

## 1. Introduction

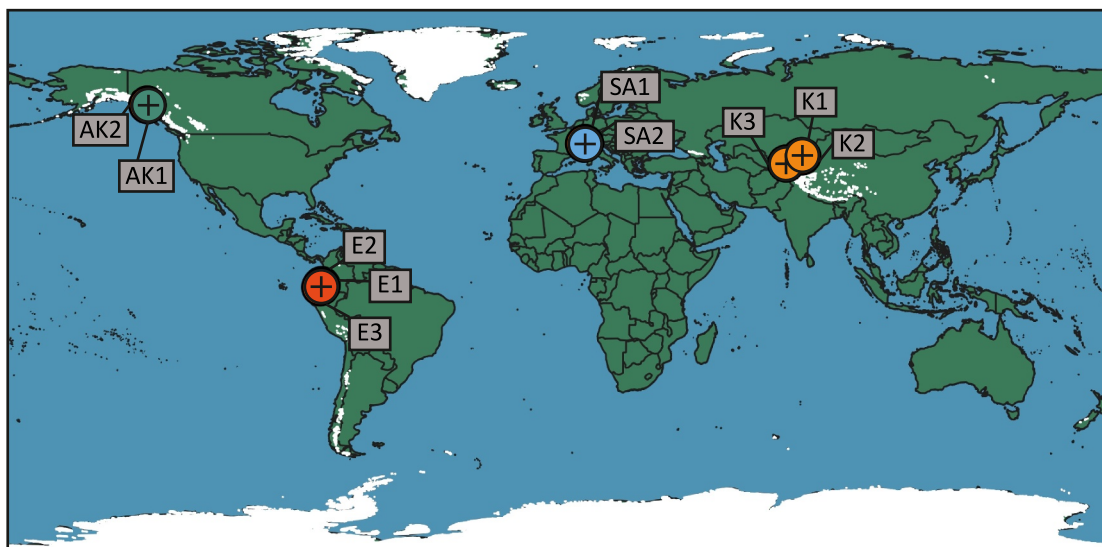
Atmospheric deposition is a ubiquitous, yet elusive, input of organic matter (OM) to the Earth's ecosystems (Bauters et al., 2018; Budhavant et al., 2023; Xenopoulos et al., 2021). Glacier ecosystems provide a unique opportunity to assess the quality and fate of atmospherically derived dissolved organic matter (DOM) because, unlike in other environments, OM deposited on glacier surfaces is not masked by large OM reservoirs (e.g., from soils; Holt, Fellman, et al., 2021; Stubbins, Hood, et al., 2012; Tranter, 2012). Previous studies showed dissolved organic carbon (DOC) in glacier outflows to be low in concentration (0.1–3.4 mg C L<sup>-1</sup>), ancient ( $\Delta^{14}\text{C}$ -DOC - 870 to -108‰, ~1,300–18,200 yBP), highly biolabile, and associated with low aromaticity DOM; thus, containing few condensed aromatic (i.e., dissolved black carbon) moieties and a high relative abundance (RA) of aliphatic (i.e., energy-rich) DOM compounds compared to neighboring non-glacial watersheds (Andrews et al., 2018; Csank et al., 2019; Holt, Fellman, et al., 2021, 2024; Hood et al., 2009, 2015; Kellerman et al., 2021).

This distinct quality of glacier-derived DOM likely renders it important in downstream biogeochemical cycling by providing a carbon subsidy to aquatic food webs (Arimitsu et al., 2018; Fellman, Hood, Raymond, Hudson, et al., 2015; Hågvær & Ohlson, 2013). A significant fraction of glacier DOM has been suggested to be derived from photodegraded fossil fuel black carbon (BC) and combustion byproducts, and thus anthropogenic aerosols are likely important drivers of carbon cycling in glacier ecosystems (Holt, Kellerman, et al., 2021, 2024; Stubbins, Hood, et al., 2012). Although visible in glacier systems, deposition of anthropogenic aerosols is a global phenomenon. Therefore, the degradation of atmospherically derived DOM across Earth's ecosystems may represent a significant, yet poorly constrained, flux of anthropogenic carbon (Singer et al., 2012; Stubbins, Hood, et al., 2012). In this context, glaciers can serve as sentinel ecosystems for constraining the impact of anthropogenic aerosols on global biogeochemical cycles (Stubbins, Hood, et al., 2012).

The importance of anthropogenic aerosols in driving glacier DOM quality is heavily debated (Bhatia et al., 2013; Fellman, Hood, Raymond, Stubbins, & Spencer, 2015; Holt et al., 2024; Li et al., 2018; Singer et al., 2012; Spencer, Guo, et al., 2014; Spencer, Vermilyea et al., 2014; Stubbins et al., 2012). The contribution of these aerosols to bulk DOM in glacier rivers has primarily been explored in southeast Alaska and Tibet, regions thought to receive fossil fuel BC from industrialized Asia (e.g., Fellman, Hood, Raymond, Stubbins, & Spencer, 2015; Li et al., 2016, 2018; Spencer, Guo, et al., 2014; Spencer, Vermilyea et al., 2014; Stubbins et al., 2012). Across glacier ecosystems, molecular-level DOM properties and carbon isotopic signatures of DOC are subtly variable, suggesting spatiotemporal variability in organic carbon (OC) source (e.g., Holt et al., 2024; Kellerman et al., 2021; Singer et al., 2012). Besides anthropogenic aerosols, allochthonous sources of OM to glacier surfaces may include pollen, local vegetation, proglacial soils and long-range atmospheric transport of dust (Antony et al., 2014; Feng et al., 2020; Holt, Kellerman, et al., 2021; Singer et al., 2012). Alternatively, DOM may originate from in situ leaching of OM beneath the glacier and autochthonous production derived from microbial activity (Bhatia et al., 2013; Holt et al., 2024; Lawson et al., 2014; Musilova et al., 2017). Globally, there is significant spatial variability in the magnitude and source (i.e., vegetation fires, biofuels vs. fossil fuels) of BC emissions (Sato et al., 2003), which may lead to variability in quantity and quality of atmospherically deposited DOM to glaciers, and broadly to Earth's ecosystems (e.g., Bauters et al., 2018; Budhavant et al., 2023; Khan et al., 2017; Li et al., 2018). Thus, the importance of anthropogenic deposition in driving DOM quality in glacier ecosystems likely varies globally, although studies to this end are few.

Fossil fuel combustion and vegetation fires have been suggested as the dominant source of dissolved BC (DBC) in different glaciers (e.g., Ding et al., 2015; Gul et al., 2021; Khan et al., 2017; Li et al., 2016; Magalhães et al., 2019). However, spatial assessments of variability in DBC sources between glacierized regions are limited (c.f., Khan et al., 2017), and BC source appointment has often relied on satellite observations or chemical transport models rather than direct measurements (e.g., Antony et al., 2014; Gul et al., 2021; Magalhães et al., 2019). Thus, the sources of DBC to glacierized regions remain poorly constrained. Furthermore, since research has focused primarily on the role of DBC in lowering glacier albedo (e.g., Bonilla et al., 2023; Khan et al., 2016, 2017; Nagorski et al., 2019), its influence on biogeochemistry is not well understood (c.f., Ding et al., 2015). DBC and its degradation byproducts may form a significant component of glacier DOM (Holt, Kellerman, et al., 2021; Stubbins, Hood, et al., 2012), but it remains unclear how this pyrogenic fraction relates to and influences the composition of the broader DOM pool.

Here, relationships between glacier DBC and DOC source were assessed to ascertain whether the deposition of anthropogenic aerosols is a global or region-specific driver of DOM composition exported from glacier ecosystems. Samples were taken from 10 glacier outflow streams across four regions (Alaska, Switzerland, Kyrgyzstan, and Ecuador; Figure 1). For the first time, compound-specific stable carbon isotopic analyses were used to constrain sources of DBC in glacier outflows (Wagner et al., 2017). To understand the relationship between DBC composition and the broader glacier DOM pool, DBC isotopic data (i.e.,  $\delta^{13}\text{C}$ -DBC) were used in conjunction with stable and radiocarbon isotopes of DOC ( $\delta^{13}\text{C}$ -DOC and  $\Delta^{14}\text{C}$ -DOC), and molecular-level DOM compositional analysis from ultrahigh resolution Fourier transform ion cyclotron resonance mass spectrometry (FT-ICR MS). Together, these data provide a global perspective on the diversity of BC and OM sources to glaciers, examining the importance of anthropogenic deposition in the glacier carbon cycle.



**Figure 1.** Study sites from 2020 to 2021 field campaigns. Sample regions are abbreviated: Alaska (AK), Switzerland (SA), Kyrgyzstan (K) and Ecuador (E). Map data: Natural Earth.

## 2. Materials and Methods

### 2.1. Study Sites, Sample Collection and Processing

Samples were collected from glacier outflow streams ( $n = 10$ ) across Southeast Alaska (USA), Switzerland, Kyrgyzstan, and Ecuador (Table S1 and Figure 1), as part of a global sampling campaign (Vanishing Glacier Project; Holt et al., 2024). Besides Ecuador, samples were taken between late-July and early September during the height of the northern hemisphere glacier melt season (Table S1). Ecuadorian samples were taken in February 2020 since proximity to the equator results in year-round ablation and thus relatively constant discharge (Table S1; Rabatel et al., 2013). In each region, sampling lasted a period of days to weeks and each glacier was sampled once (Table S1). Therefore, DBC, DOC and DOM composition reflected that of the sampling period and does not assess temporal gradients in source that may exist at each site.

At each site, samples were collected and immediately filtered into pre-rinsed (three times with filtrate) and acid-washed (10% HCl v/v) polycarbonate bottles or acid-washed and combusted (5h, 550°C) amber glass vials. Samples for DOC analysis were filtered to 0.7  $\mu\text{m}$  using ashed (5 hr, 450°C) GF/F filters. Samples for DBC were filtered using trace metal grade Geotech Polyethersulfone dispos-a-filter™ capsules (0.45  $\mu\text{m}$ ). FT-ICR MS and DOC carbon isotope samples were also filtered to 0.45  $\mu\text{m}$  in all sites except Ecuador, where samples were filtered to 0.7  $\mu\text{m}$ . All samples were acidified (pH 2, 10 M HCl) and stored frozen (−20°C) in the dark until subsequent preparation and analysis. Milli-Q water was taken to field sites and treated following the same sampling, processing, and storage protocols as the samples. Field blanks showed no evidence of contamination, as confirmed by DOC concentration and molecular-level analyses.

Samples for DBC and FT-ICR MS analyses were solid phase extracted (SPE). Briefly, Bond Elut PPL cartridges were conditioned sequentially with high performance liquid chromatography (HPLC) grade MeOH, Milli-Q, MeOH and pH 2 Milli-Q (10 M HCl). Subsequently, to isolate DOC for DBC and FT-ICR MS analyses 6–15 and 1 L of acidified filtrate were extracted onto 1 g (6 mL) and 100 mg (3 mL) PPL cartridges, respectively (Dittmar et al., 2008). Following extraction, PPL cartridges were rinsed with two cartridge volumes of pH 2 Milli-Q (10 M HCl), dried with a flow of ultrahigh purity nitrogen gas (Dittmar et al., 2008), and stored frozen (−20°C) in the dark until analysis.

### 2.2. Dissolved Organic Carbon Quantification and Carbon Isotopic Analysis

For Alaskan, Ecuadorian, and Swiss samples, DOC concentrations were measured on a Shimadzu TOC-L<sub>CPH/CPN</sub> analyzer following standard methods (Stubbins & Dittmar, 2012). Samples from Kyrgyzstan were measured on a GE Sievers M9 TOC analyzer (Boix Canadell et al., 2021). Concentrations were calculated based on replicate

measurements, with a coefficient of variance <2%. Streams were analyzed for stable and radiogenic carbon isotopes of DOC (i.e.,  $\delta^{13}\text{C}$ -DOC and  $\Delta^{14}\text{C}$ -DOC). In brief, DOC was UV-oxidized and evolved  $\text{CO}_2$  purified, trapped cryogenically, and analyzed for  $\Delta^{14}\text{C}$  at the National Ocean Sciences Accelerator Mass Spectrometry Facility at Woods Hole Oceanographic Institution, USA (Xu et al., 2021). A split of  $\text{CO}_2$  was measured for  $\delta^{13}\text{C}$ -DOC on a stable isotope ratio mass spectrometer (IRMS; Xu et al., 2021). Estimated relative contributions of DOC from fossil fuels versus contemporary OC sources were calculated using the following isotopic mass-balance equation:

$$\Delta^{14}\text{C}_{\text{sample}} = \Delta^{14}\text{C}_{\text{bio}} \times f_{\text{bio}} + \Delta^{14}\text{C}_{\text{fossil}} \times (1 - f_{\text{bio}}) \quad (1)$$

where  $\Delta^{14}\text{C}_{\text{sample}}$  represents the measured isotopic signature of the sample,  $\Delta^{14}\text{C}_{\text{bio}}$  is assumed to be between 10 and 105‰ based previous published data for C3 and C4 vegetation and  $\Delta^{14}\text{C}_{\text{fossil}}$  is −1,000‰ (Budhavant et al., 2023). The range of isotopic values for  $\Delta^{14}\text{C}_{\text{bio}}$  was used to allow for variability in  $\Delta^{14}\text{C}$  of contemporary sources due to the decay of  $^{14}\text{C}$  since the bomb-spike.

### 2.3. Dissolved Black Carbon Quantification and Stable Carbon Isotopic Analysis

Glacier streamwater DBC concentrations were quantified, and stable isotopic signatures assessed, using the benzenepolycarboxylic acid (BPCA) method (Wagner et al., 2017). Briefly, dry 1 g PPL cartridges were eluted with MeOH. Eluate volumes equating to 0.5 mgC were placed into ashed (5 hr, 550°C) 2 mL glass ampules and MeOH evaporated to dryness. Concentrated  $\text{HNO}_3$  (0.5 mL; 15.8 N) was added to each ampule, and subsequently flame-sealed and heated (6 hr, 160°C) to oxidize condensed aromatic DOM to BPCAs. After oxidation, ampules were opened, the reaction mixture evaporated to dryness (60°C, under flow of nitrogen gas) and BPCA-containing residues re-dissolved in dilute  $\text{H}_3\text{PO}_4$  (0.6 M) for subsequent quantitative analyses (Wagner et al., 2017).

Using HPLC (Thermo Fisher UltiMate 3,000 equipped with a diode array detector), individual BPCAs were distinguished based on retention time, and concentration quantified based on calibration curves for commercially available standards (TCI America; Wagner et al., 2017). Benzenepentacarboxylic acid (B5CA) and benzenhexacarboxylic acid (B6CA) were separated on an Agilent Poroshell 120 phenyl-hexyl column (4.6 × 150 mm, 2.7  $\mu\text{m}$ ) using an aqueous gradient of  $\text{H}_3\text{PO}_4$  (0.6 M; pH 1) and  $\text{Na}_3\text{PO}_4$  (20 mM; pH 6) buffer (Wagner et al., 2017). Sample DBC concentrations were calculated using the established power relationship between DBC ( $\mu\text{M-C}$ ) and the sum of B6CA and B5CA (nm-BPCA;  $n = 352$ ,  $R^2 = 0.998$ ,  $p$ -value < 0.0001; Stubbins et al., 2015):

$$[\text{DBC}] = 0.0891 \times ([\text{B6CA} + \text{B5CA}])^{0.9175} \quad (2)$$

Here, both raw BPCA quantities and estimated DBC concentrations were reported to facilitate comparison between studies.

Compound-specific  $\delta^{13}\text{C}$  values for individual BPCAs were measured using a Dionex Ultimate 3000 HPLC connected to a Delta V IRMS via an LC Isolink interface following methods detailed previously (Wagner et al., 2017). Online oxidation quantitatively converts BPCAs to  $\text{CO}_2$ , which is subsequently extracted from the mobile phase for detection by IRMS. Sample BPCA-specific  $\delta^{13}\text{C}$  values were corrected using the isotopic composition of calibrated B5CA and B6CA standards (Wagner et al., 2017). Standard deviations applied to corrected sample  $\delta^{13}\text{C}$  values were propagated to account for errors associated with replicate standard and sample BPCA measurements (Wagner et al., 2017). The BPCA-specific  $^{13}\text{C}$  content is expressed in  $\delta^{13}\text{C}$  per mil (‰) notation relative to Vienna Pee Dee Belemnite. The error associated with corrected  $\delta^{13}\text{C}$  values was <0.4‰.

### 2.4. Fourier Transform Ion Cyclotron Resonance Mass Spectrometry

Dried 100 mg PPL cartridges were eluted with HPLC grade MeOH into 2 or 4 mL ashed (5h, 550°C) glass vials. The volume of MeOH used was adjusted dependent on the DOC concentration of the sample to achieve a target eluent concentration of 50  $\mu\text{g C mL}^{-1}$ . MeOH extracts were stored frozen (−20°C) in the dark until analysis.

The SPE extracts of DOM were analyzed with a custom-built hybrid linear ion trap FT-ICR mass spectrometer equipped with a 21 T superconducting solenoid magnet (Hendrickson et al., 2015; Smith et al., 2018). Typical

**Table 1**

*Concentrations and Carbon Isotopes ( $\delta^{13}\text{C}$  and  $\Delta^{14}\text{C}$ ) for Dissolved Organic Carbon (DOC) and Estimated Fossil Fuel Derived Fraction of DOC, As Well As Dissolved Black Carbon (DBC) Concentration, DBC/DOC (%), and Concentrations and Stable Carbon Isotopes for Benzenepolycarboxylic Acid (BPCA; B5CA and B6CA) Molecular Markers*

Region	Alaska		Switzerland		Kyrgyzstan			Ecuador		
Sample ID	AK1	AK2	SA1	SA2	K1	K2	K3	E1	E2	E3
DOC ( $\text{mg C L}^{-1}$ )	0.3	0.4	0.3	0.5	0.2	0.4	0.3	1.1	0.6	0.3
$\delta^{13}\text{C-DOC}$ (‰)	−26.0	−28.0	−27.2	−26.7	−25.4	−25.2	−24.1	−20.5	−21.3	−22.7
$\Delta^{14}\text{C-DOC}$ (‰)	−896.9	−810.1	−442.1	−500.4	−495.1	−349.2	−510.4	−114.5	−195.1	−179.5
Age (yBP)	18,200	13,300	4,620	5,510	5,420	3,380	5,670	910	1,680	1,520
Fraction Fossil (%)	90–91	81–83	45–50	51–55	50–54	36–41	52–56	12–20	20–27	19–26
B5CA ( $\text{ng C L}^{-1}$ )	8.77	11.65	6.13	9.49	11.65	30.03	21.26	2.40	1.32	4.44
B6CA ( $\text{ng C L}^{-1}$ )	3.72	4.92	2.04	3.12	3.96	9.01	6.73	1.20	0.84	1.68
DBC ( $\mu\text{g C L}^{-1}$ )	1.10	1.44	0.74	1.12	1.37	3.16	2.33	0.36	0.22	0.59
DBC/DOC (%)	0.37	0.36	0.25	0.22	0.69	0.79	0.78	0.03	0.04	0.20
$\delta^{13}\text{C-B5CA}$ (‰)	−27.3	−27.4	−24.9	−25.8	−24.2	−24.3	−25.7	−24.1	−21.8	−24.4
$\delta^{13}\text{C-B6CA}$ (‰)	−28.8	−28.6	−25.4	−27.3	−25.7	−26.6	−27.2	−24.7	−23.2	−23.6

conditions for negative-ion formation were: emitter voltage:  $-2.8 - 3.2$  kV; S-lens RF level: 45%; heated metal capillary temperature:  $350^\circ\text{C}$ . Time-domain transients of 3.1 s each were conditionally co-added (100 scans) with the Predator data station prior to phase-correction (Xian et al., 2010), and internal “walking” calibration with 10–15 abundant homologous series that spanned the molecular weight distribution (Savory et al., 2011). Peaks with signals greater than the root mean square baseline noise plus  $6\sigma$  were exported to a peak list, and elemental compositions assigned between 170 and 1,200 Da in PetroOrg©, within the bounds  $\text{C}_{1-100}\text{H}_{4-200}\text{O}_{1-30}\text{N}_{0-4}\text{S}_{0-2}$  (error  $\pm 0.3$  ppm; Corilo, 2014).

Assigned molecular formulae were classified according to their neutral elemental composition. Formulae that contained only C, H and O were classed as CHO-only. Where heteroatoms N and/or S were assigned, the formulae were classed as CHON, CHOS and CHONS. From elemental composition, the nominal oxidation state of carbon (NOSC), a metric used to infer biogeochemical reactivity and biolability of a compound, and modified aromaticity index ( $\text{AI}_{\text{mod}}$ ) were calculated (Koch & Dittmar, 2006, 2016; Riedel et al., 2012). Based on  $\text{AI}_{\text{mod}}$  (i.e., aromaticity), and elemental ratios (H/C and O/C) formulae were categorized into four compound classes to infer structure: polyphenolic and condensed aromatics ( $\text{AI}_{\text{mod}}$  values of 0.5–0.67 and  $> 0.67$ , respectively), highly unsaturated and phenolic (HUP;  $\text{AI}_{\text{mod}}$  of  $< 0.5$  and  $\text{H/C} < 1.5$ ), and aliphatic ( $\text{H/C} \geq 1.5$ ,  $\text{O/C} \leq 0.9$ ; includes N-containing aliphatics). Compound classes were purely operational since specific structural configurations cannot be derived from FT-ICR MS and elemental composition alone; thus, each formula may represent numerous structural isomers (Koch & Dittmar, 2006). The RA of assigned formulae was calculated as the contribution of a peak as a fraction of the total intensity of all assigned peaks in a sample scaled to 10,000.

## 2.5. Statistical Analysis

Principal component (PC) analysis was used to connect major bulk DOC properties and molecular-level DOM composition to the quantities and stable isotopic signatures of DBC. This provided insight into the diversity of DOM and DBC sources available to glaciers, as well as how DOM and DBC composition covary. The PC analysis considered concentrations of DOC, DBC and individual measured BPCAs, together with the ratio of DBC to DOC, carbon isotopic signatures (i.e.,  $\Delta^{14}\text{C-DOC}$ ,  $\delta^{13}\text{C-DOC}$ ,  $\delta^{13}\text{C-B5CA}$  and  $\delta^{13}\text{C-B6CA}$ ; Table 1) and RA weighted FT-ICR MS metrics (i.e., mass, elemental ratios, NOSC,  $\text{AI}_{\text{mod}}$ , heteroatom classes and compound classes; Table 2).



**Table 2**

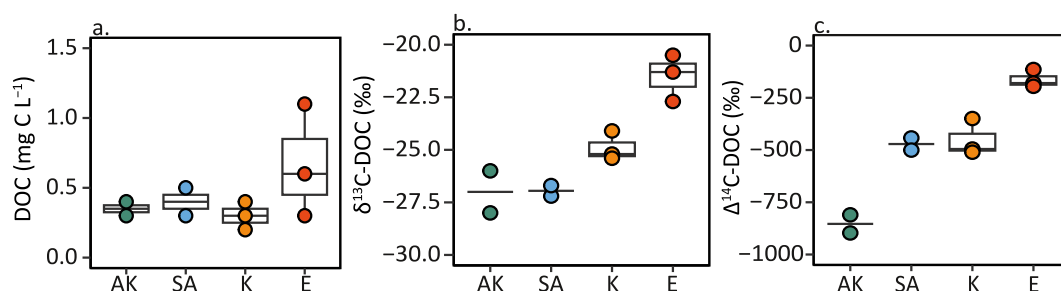
Number of Formulae and Mean Relative Abundance (RA) Weighted Mass, Atomic Ratios, Nominal Oxidation State of Carbon (NOSC) and Modified Aromaticity Index ( $AI_{mod}$ ), Together With the Percent RA (%RA) of Heteroatom and Compound Classes

Region	Alaska		Switzerland		Kyrgyzstan			Ecuador		
Sample ID	AK1	AK2	SA1	SA2	K1	K2	K3	E1	E2	E3
Formulae (#)	7,750	10,138	11,267	11,406	8,263	16,979	12,676	3,974	6,998	8,075
Mass (Da)	455.7	440.2	426.1	454.7	413.1	482.8	451.8	452.6	477.4	458.8
H/C	1.33	1.34	1.36	1.36	1.46	1.35	1.37	1.5	1.44	1.45
O/C	0.46	0.47	0.46	0.46	0.4	0.47	0.45	0.42	0.43	0.41
NOSC	−0.35	−0.36	−0.38	−0.38	−0.51	−0.33	−0.39	−0.62	−0.51	−0.56
$AI_{mod}$	0.2	0.2	0.19	0.18	0.15	0.18	0.18	0.12	0.14	0.14
CHO (%RA)	74.7	76.5	70.7	69.1	47.9	60	68.6	67.9	42.6	58.8
CHON (%RA)	24.2	21.1	18.2	22.2	46.7	31.3	25.2	9.5	10.5	15.6
CHOS (%RA)	1.1	2.4	10.1	7.9	4.5	6.9	5.8	21.4	44.8	22.8
CHONS (%RA)	0	0	1.1	0.8	0.9	1.8	0.4	1.1	2.1	2.8
Highly unsaturated and phenolic (%RA)	68.6	65.5	67.5	68.2	48.9	70.6	60.6	39.7	52.5	50.2
Aliphatic (%RA)	26.9	29.8	29.6	29.3	49.3	26.9	35.4	58.4	45.0	47.9
Polyphenolics (%RA)	3.8	3.9	2.3	2.0	1.4	2.0	3.1	1.7	2.0	1.6
Condensed Aromatics (%RA)	0.8	0.8	0.5	0.3	0.4	0.4	0.9	0.1	0.1	0.1

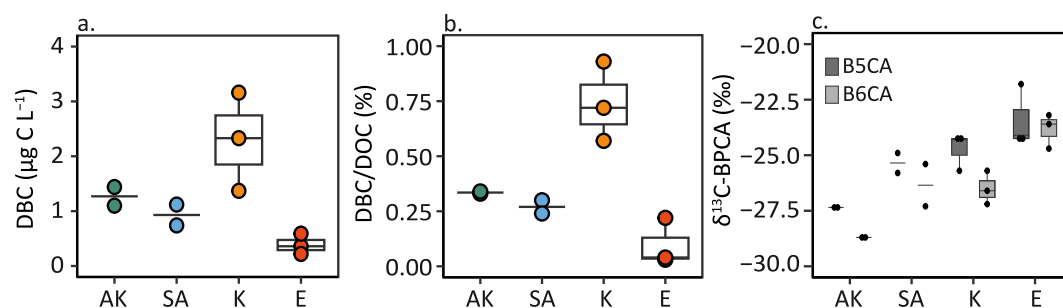
### 3. Results and Discussion

#### 3.1. Bulk Dissolved Organic Carbon Quantities and Carbon Isotopic Signatures

Glacier outflow DOC concentrations ranged between 0.2 and 1.1 mg C L<sup>−1</sup> (median 0.4 mg C L<sup>−1</sup>; Table 1; Figure 2a), consistent with reported concentrations for glacier ecosystems globally (0.1–3.4 mg C L<sup>−1</sup>; Hood et al., 2015; Holt et al., 2024). Besides sample E1, which had the highest measured DOC concentration of all regions, DOC had a narrow range of concentrations (0.2–0.6 mg C L<sup>−1</sup>; Table 1; Figure 2a). Median  $\delta^{13}\text{C}$ -DOC and  $\Delta^{14}\text{C}$ -DOC were −25.3‰ and −468.6‰, respectively (Table 1; Figures 2b and 2c). Globally, outflow DOC has previously been shown to be variably aged ( $\Delta^{14}\text{C}$ -DOC −896.9 to −108‰) with  $\delta^{13}\text{C}$ -DOC signatures ranging from −30 to −20.5‰ (Andrews et al., 2018; Csank et al., 2019; Holding et al., 2017; Holt et al., 2024; Hood et al., 2009). Our study covered a similar range in carbon isotopic signatures ( $\delta^{13}\text{C}$ -DOC −28.0 to −20.5‰ and  $\Delta^{14}\text{C}$ -DOC −896.9 to −114.5‰; Table 1 and Figures 2b and 2c). There was overlap in  $\delta^{13}\text{C}$ -DOC and  $\Delta^{14}\text{C}$ -DOC signatures between sites in different regions, with the Alaskan and Ecuadorian glaciers forming the lower (i.e., <sup>13</sup>C and <sup>14</sup>C depleted) and upper (i.e., <sup>13</sup>C and <sup>14</sup>C enriched) extremes of the ranges, respectively (Table 1; Figures 2b and 2c).



**Figure 2.** (a) Dissolved organic carbon (DOC) concentration and (b, c) bulk carbon isotope data ( $\delta^{13}\text{C}$ -DOC and  $\Delta^{14}\text{C}$ -DOC). Boxplots show the minimum, maximum and median values as well as the interquartile range. Where  $n = 2$  the solid black line indicates the median. Individual data points are plotted on top of boxplots. Sample regions are abbreviated: Alaska (AK), Switzerland (SA), Kyrgyzstan (K) and Ecuador (E).



**Figure 3.** (a) Dissolved black carbon (DBC) concentration, (b) percentage of dissolved organic carbon (DOC) that is DBC, and (c)  $\delta^{13}\text{C}$  of benzenepentacarboxylic (B5CA) and hexacarboxylic (B6CA) acid (i.e.,  $\delta^{13}\text{C}$ -BPCA signature). Boxplots show the minimum, maximum and median values as well as the interquartile range. Where  $n = 2$  the solid black line indicates the median. Individual data points are plotted on top of boxplots. Sample regions are abbreviated: Alaska (AK), Switzerland (SA), Kyrgyzstan (K) and Ecuador (E).

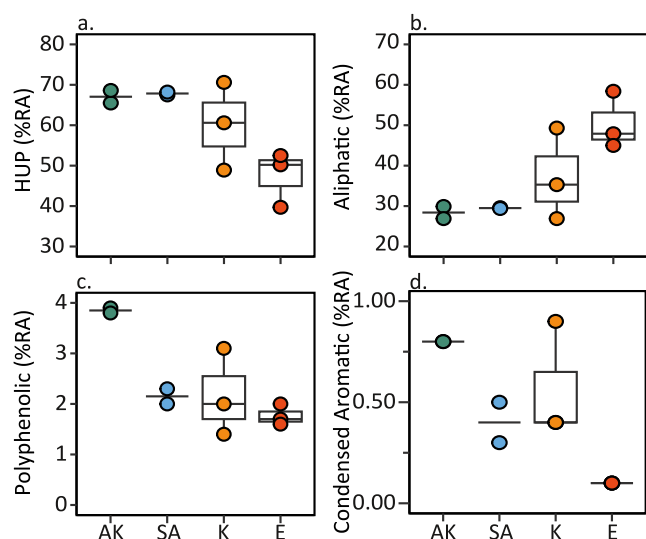
### 3.2. Dissolved Black Carbon Quantities and Stable Carbon Isotopic Signatures

The concentrations of DBC molecular markers, B5CA and B6CA, were variable across glacier outflows, with consistently higher concentrations of B5CA than B6CA (median  $9.13 \pm 8.9$  and  $3.42 \pm 2.6$  ng C L<sup>-1</sup>, respectively; Table 1). Estimated DBC concentrations ranged from 0.22 to  $3.16 \mu\text{g C L}^{-1}$  (E2 and K2, respectively; median  $1.11 \mu\text{g C L}^{-1}$ ; Table 1 and Figure 3a). The proportion of DOC which was DBC ranged from 0.03% to 0.79% (median 0.31% of DOC; Table 1 and Figure 3b). Glacier outflow DBC constitutes a substantially lower proportion of DOC than in non-glacier rivers (2.5%–12.2% of DOC) since glaciers receive DBC solely from atmospheric deposition, whereas DBC in non-glacier rivers is largely derived from catchment sources, such as leaching of BC from burnt biomass and soil OM (Jaffé et al., 2013; Wagner et al., 2018). Concentrations of DBC were below those reported for non-glacial rivers (18–1,700  $\mu\text{g C L}^{-1}$ ; Jaffé et al., 2013), and at the lower end of the range observed in glacier ecosystems, including the surface (e.g., supraglacial snow, melt streams and ponds) and proglacial lakes and rivers (0.53–177  $\mu\text{g C L}^{-1}$ ; 0.001%–3.7% of DOC; Ding et al., 2015; Khan et al., 2017). Here, glacier DBC concentrations and relative contributions of DBC to the DOC pool were more comparable to those observed in the open ocean (1–19  $\mu\text{g C L}^{-1}$  and 0.1%–4.7% of DOC, respectively; Wagner et al., 2018), where atmospheric deposition is also likely an important BC source (Wagner et al., 2019).

The compound-specific stable carbon isotopic signatures of DBC in glacier outflows showed that  $\delta^{13}\text{C}$ -B5CA and  $\delta^{13}\text{C}$ -B6CA (median  $-24.7$  and  $-26.2$ ‰ respectively) were similar to  $\delta^{13}\text{C}$ -DOC ( $-25.3$ ‰; Table 1, Figures 2b and 3c). Similar to  $\delta^{13}\text{C}$ -DOC and  $\Delta^{14}\text{C}$ -DOC, there was a substantial range in  $\delta^{13}\text{C}$ -B5CA and  $\delta^{13}\text{C}$ -B6CA ( $-29.1$  to  $-21.8$ ‰ and  $-29.5$  to  $-23.2$ ‰, respectively) with some overlap in isotopic signatures between regions (Figure 3c). Glacier outflow  $\delta^{13}\text{C}$ -BPCA signatures spanned the range observed for the open ocean and were typically more  $^{13}\text{C}$ -enriched than that seen in non-glacial rivers (Wagner et al., 2017, 2019). The substantial range across the studied regions in glacier  $\delta^{13}\text{C}$ -BPCAs values, as well as the broad age and carbon isotopic signatures of DOC, suggests that atmospheric deposition and the contributions of OC and BC derived from fossil fuel sources likely vary across glacier outflows.

### 3.3. Molecular-Level Dissolved Organic Matter Composition

Across the data set, between 3,974 and 16,979 mass peaks were assigned formulae (median 9,201; Table 2) in mass spectra derived from negative-ion electrospray ionization 21 T FT-ICR MS. The median RA weighted mean mass of the assigned formulae was  $453.7 \pm 21.0$ , which varied moderately between glacier outflows and glacierized regions. The RA weighted mean NOSC, and elemental ratios of H/C and O/C were variable across studied regions, ranging from  $-0.62$  to  $-0.33$ , 1.33 to 1.50, and 0.40 to 0.47, respectively (Table 2). Typically, across the glacier regions studied here, the majority of the RA of assigned formulae contain only C, H and O (i.e., CHO-only compound; median 68.3% RA, range 42.6%–76.5% RA; Table 2), as expected for glacier and riverine DOM (Kellerman et al., 2021). Nevertheless, heteroatom classes, CHON and CHOS, made up a sizable, yet variable, fraction of DOM composition across the study regions (median CHON  $21.7\% \pm 10.8\%$  RA and CHOS  $7.4\% \pm 13.4\%$  RA; Table 2), consistent with past studies that have shown glacier DOM is enriched in heteroatom containing formulae compared to riverine DOM (Holt, Fellman, et al., 2021, 2024;



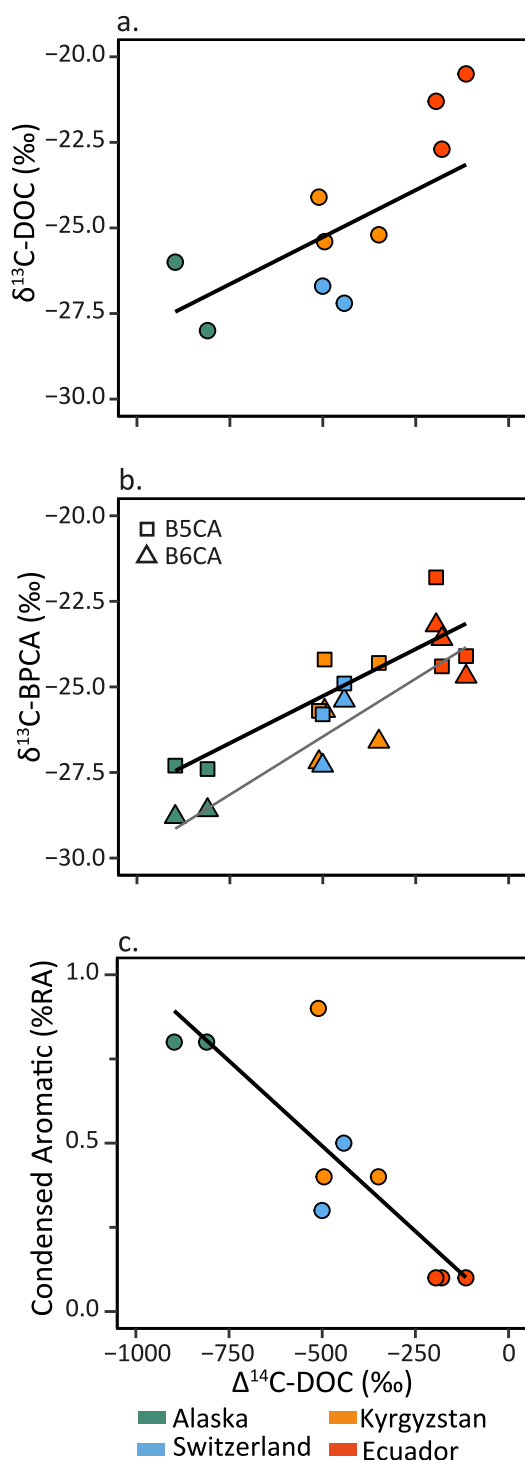
**Figure 4.** The percent relative abundance (%RA) of (a) highly unsaturated and phenolic (HUP), (b) aliphatic (includes N-containing aliphatics), (c) polyphenolic and (d) condensed aromatic formulae across study regions as determined by 21 T Fourier ion cyclotron resonance mass spectrometry (FT-ICR MS). Boxplots show the minimum, maximum and median values as well as the interquartile range. Where  $n = 2$  the solid black line indicates the median. Individual data points are plotted on top of boxplots. Sample regions are abbreviated: Alaska (AK), Switzerland (SA), Kyrgyzstan (K) and Ecuador (E).

Kellerman et al., 2021). In all glacier outflows, CHONS formulae made up <3% of RA. Overall, molecular-level DOM composition was dominated by HUP and aliphatic compounds (median 63.1% and 32.6% RA, respectively; Table 2 and Figure 4), which supports previous molecular-level studies showing that glacier DOM is enriched in aliphatic compounds compared to non-glacial rivers (e.g., Holt, Fellman, et al., 2021; Kellerman et al., 2021; Lawson et al., 2014; Singer et al., 2012). The median percent RA of polyphenolic ( $2\% \pm 0.9\%$  RA) and condensed aromatic ( $0.4\% \pm 0.3\%$  RA) formulae was low, yet variable between sites, where the RA of polyphenolics ranged from 1.4% to 3.9% and condensed aromatics from 0.1% to 0.9% (Table 2 and Figure 4). Typically, glacier river DOM is low in aromaticity, and thus exhibits a low RA of condensed aromatic and polyphenolic compounds compared to non-glacier rivers (Kellerman et al., 2021). These observations are consistent with the low quantities of DBC found in glacier environments (Table 2; Ding et al., 2015; Jaffé et al., 2013; Khan et al., 2017). Despite underlying similarities in molecular-level DOM composition of glacier outflows, there was large variability in FT-ICR MS metrics across sites, particularly in the percent RA of HUP (39.7%–70.6% RA), aliphatic (26.9%–58.4% RA) and heteroatom containing compounds (Table 2 and Figure 4), reflecting a global gradient in DOM composition (Holt et al., 2024). Overall, this variability in molecular-level DOM properties, together with carbon isotopic signature of DOC and DBC, demonstrated that DOM quality and source varied across glacier outflows, suggesting that the biogeochemical role of glacier DOM is spatially variable (Holt et al., 2024).

### 3.4. Spatial Variability in Dissolved Organic Matter and Black Carbon Source: Implications for Glacier Carbon Cycling

Across glacier regions, the age of streamwater DOC (i.e.,  $\Delta^{14}\text{C}$ -DOC) was significantly correlated with  $\delta^{13}\text{C}$ -DOC,  $\delta^{13}\text{C}$ -B5CA and  $\delta^{13}\text{C}$ -B6CA, as well as condensed aromatic % RA as determined by FT-ICR MS (Figure 5). Enrichment in  $^{14}\text{C}$ -DOC was correlated with  $^{13}\text{C}$  enrichment in bulk DOC, B5CA, and B6CA ( $R^2 = 0.57, 0.68$  and  $0.79$  respectively, and  $p$ -values  $< 0.01$ ; Figures 5a and 5b), which indicated that younger DOC was associated with isotopically enriched OC and BC sources, such as material from C4 plants and/or microbial biomass. Concomitantly,  $\Delta^{14}\text{C}$  values of streamwater DOC were significantly negatively correlated to the % RA of condensed aromatic compounds ( $R^2 = 0.69$  and  $p$ -value  $< 0.01$ ; Figure 5c), meaning that older glacial DOC had a greater proportion of highly aromatic and perhaps soot-like molecular formulae. To comprehensively assess this covariance in  $\Delta^{14}\text{C}$ -DOC with DOC and DBC stable carbon isotopes, and molecular-level DOM properties (Figure 5), a PC analysis was conducted that included quantities and isotopic signatures of DOC and DBC, together with molecular-level DOM compositional metrics (Figure 6a). PC1 explained 61.3% of the variability in the data set and was strongly positively correlated with FT-ICR MS metrics related to aromaticity (e.g.,  $\text{AI}_{\text{mod}}$  and NOSC) and % RA of condensed aromatic compounds. PC1 was strongly negatively associated with high H/C ratios and % RA of aliphatic and CHOS compounds, together with  $^{14}\text{C}$ -DOC,  $^{13}\text{C}$ -DOC,  $^{13}\text{C}$ -BPCA enrichment (Figure 6a), suggesting that younger DOC was derived from  $^{13}\text{C}$ - and aliphatic-enriched sources. Furthermore, significant positive correlations between  $\delta^{13}\text{C}$ -DOC and  $\delta^{13}\text{C}$ -BPCA ( $R^2 = 0.45$  and  $0.49$  for B5CA and B6CA, respectively, and  $p$ -values  $< 0.05$ ) suggest isotopically similar sources for DOC and DBC, which is consistent with a component of glacier outflow DOM being of atmospheric origin (e.g., Stubbins, Hood, et al., 2012). Ecuadorian and Alaskan outflows occupied the negative and positive extremes of PC1, respectively (Figure 6b). Glacier outflows in Switzerland and Kyrgyzstan were typically positioned at positive values of PC1, closer and thus compositionally more aligned with Alaskan samples compared to outflows in Ecuador (Figure 6b). This gradient between molecular and isotopic composition indicates that atmospheric deposition and source partly controls glacier outflow DOM composition, and likely exists due to the spatially heterogeneous nature of emissions and BC sources across the planet (Holt et al., 2024; Sato et al., 2003).

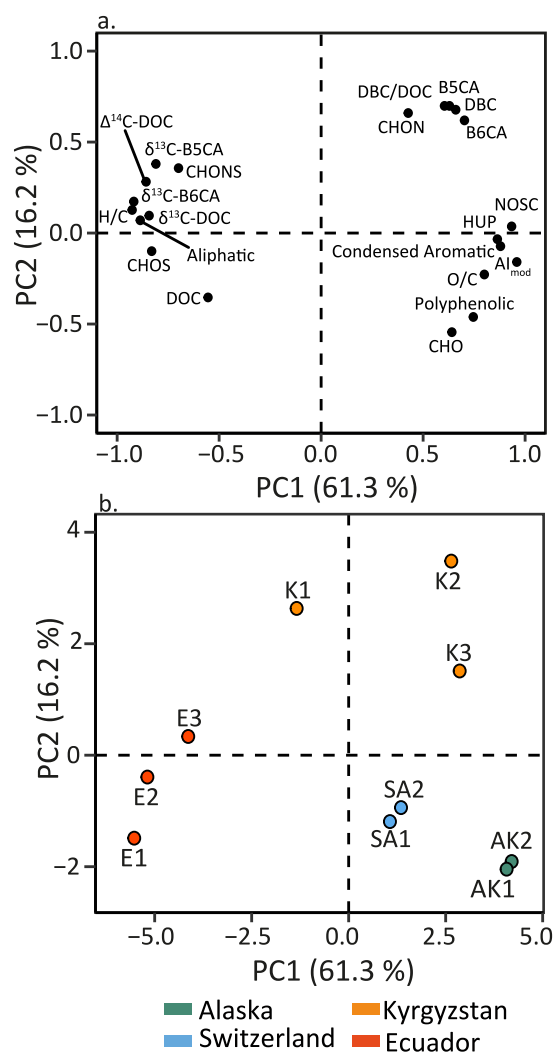




**Figure 5.** Relationship between  $\Delta^{14}\text{C}$ -DOC and (a)  $\delta^{13}\text{C}$ -DOC (b)  $\delta^{13}\text{C}$ -B5CA and  $\delta^{13}\text{C}$ -B6CA, and (c) % relative abundance (RA) of condensed aromatic compounds, respectively. (b) Solid black and gray lines indicate the respective linear regressions for  $\delta^{13}\text{C}$ -B5CA and  $\delta^{13}\text{C}$ -B6CA. Individual data points are colored and shaped according to the region and molecular marker, respectively—see panel for details.

PC2 explained 16.2% of the variability in the data set and was primarily driven by the B5CA, DBC concentration as well as % RA of CHON (Table 2 and Figure 6a). Outflow samples in Kyrgyzstan accounted for a substantial portion of variability in PC2 since they exhibited CHON enrichment in comparison to other regions and one outflow sample (K2) had a far greater concentration of B5CA and thus DBC ( $30.03$  and  $3.16 \mu\text{g C L}^{-1}$ , respectively) compared to the median ( $9.13$  and  $1.11 \mu\text{g C L}^{-1}$ , respectively; Table 1, Figure 6). The variability along PC2 may be related to residence time of DOM on the glacier surface influencing the degree of bio- and photodegradation, processes shown to influence the heteroatom content of the DOM pool (Antony et al., 2018; Holt, Kellerman, et al., 2021), and also intrinsic differences in OM quality related to source material, degree of charring, and solubility (Wagner et al., 2018).

The gradient in glacier outflow molecular-level and carbon isotopic signatures is likely partly driven by the source and quality of atmospheric deposition (Figures 5 and 6). In particular, the concomitant decrease in  $\delta^{13}\text{C}$ -DOC,  $\delta^{13}\text{C}$ -DBC, and  $\Delta^{14}\text{C}$ -DOC values is consistent with a predominance of deposition from radiocarbon-dead fossil fuel combustion byproducts, while enrichment in  $^{13}\text{C}$  and  $^{14}\text{C}$  is consistent with a greater proportion of contemporary OC sources (e.g., OC and BC from vegetation fires and biofuels, or OC from in situ production). This is in agreement with studies showing that Ecuadorian glaciers receive OM from biogenic and biomass burning emissions from Amazon rainforest and associated ecotones (Ginot et al., 2002), whilst catchments in southeast Alaska have been highlighted as likely receiving anthropogenic deposition from local sources and from East Asia (including fossil fuel derived BC; Fellman, Hood, Raymond, Stubbins, & Spencer, 2015; Nagorski et al., 2019; Stubbins, Hood, et al., 2012; Yu et al., 2012). The  $\delta^{13}\text{C}$  signatures of B5CA, B6CA, and DOC from modern C3 plant chars have been shown to be on average  $-26.9$ ,  $-27.2$  and  $-26.7\text{‰}$  respectively (Kohn, 2010; Wagner et al., 2017; Yarnes et al., 2011). As expected,  $\delta^{13}\text{C}$ -B5CA and  $\delta^{13}\text{C}$ -B6CA of modern C4 chars ( $-13.8$  and  $-13.7\text{‰}$ , respectively) have more  $^{13}\text{C}$ -enriched signatures than C3 chars since their parent material is  $^{13}\text{C}$ -enriched ( $-14$  to  $-10\text{‰}$  compared to  $-37$  to  $-20\text{‰}$  respectively; Cerling et al., 1997; Kohn, 2010; Vaezzadeh et al., 2021; Yarnes et al., 2011). Therefore, the variability in  $\delta^{13}\text{C}$  values across the data set, particularly of younger and  $^{13}\text{C}$ -enriched outflows (e.g., in Ecuador, or between sites in Switzerland and Kyrgyzstan), could in part be explained by a changing dominance and source of emissions from C3 to C4 vegetation. Post-depositional photodegradation of OC can result in an aliphatic-rich signature of glacier DOM and enriched  $\delta^{13}\text{C}$ -DOC values (Holt, Kellerman, et al., 2021; Spencer et al., 2009). Thus, photodegraded plant material and combustion byproducts (i.e., photodegraded C3, C4 or C3/C4 mix) could explain the range in stable carbon isotopic composition seen across these glacier outflows, as well as the exceptionally aliphatic-rich composition seen in  $^{13}\text{C}$  enriched sites. Although significant correlations between bulk DOC and DBC specific markers suggest that a fraction of glacier DOC is from atmospheric deposition (Figures 5 and 6), it is likely that a component of modern DOC and aliphatic-rich DOM is derived from contemporary microbial production, as suggested previously (Holt et al., 2024; Lawson et al., 2014; Musilova et al., 2017). Positive correlations between  $\Delta^{14}\text{C}$ -DOC and  $\delta^{13}\text{C}$  values suggest that a modern microbial source would likely have  $^{13}\text{C}$ -enriched DOC signatures, and be more prominent in glacier environments (e.g.,



**Figure 6.** (a, b) Principal component (PC) analysis for glacier outflow samples. PC analysis considered relative abundance (RA) weighted FT-ICR MS metrics, dissolved organic carbon (DOC), dissolved black carbon (DBC) and molecular marker (B5CA and B6CA) concentrations, together with carbon isotopic signatures ( $\Delta^{14}\text{C-DOC}$ ,  $\delta^{13}\text{C-DOC}$ ,  $\delta^{13}\text{C-B5CA}$  and  $\delta^{13}\text{C-B6CA}$ ). Modified aromaticity index and nominal oxidation state of carbon are abbreviated to  $\text{AI}_{\text{mod}}$  and  $\text{NOSC}$ , respectively.

those in Ecuador) receiving atmospheric inputs from burnt contemporary sources (Figure 5).

Conversely, the positive correlation between  $\Delta^{14}\text{C-DOC}$  and  $\delta^{13}\text{C-DOC}$ , together with  $\delta^{13}\text{C-BPCAs}$ , suggests that glacier DOC with the lowest  $\delta^{13}\text{C}$  values were derived from ancient material and not from modern sources (e.g., vegetation fires or in situ microbial production; Figure 5). Fossil fuels are radiocarbon-dead and  $\delta^{13}\text{C}$  signatures of B5CA, B6CA and DOC from crude oils have been shown to be on average  $-28.0$ ,  $-28.7$  and  $-27.8\text{‰}$ , respectively (Goranov et al., 2021). Thus, fossil fuel combustion byproducts may explain the relatively old and  $^{13}\text{C}$ -depleted isotopic signatures across these glacier environments, with the most pronounced fossil fuel-derived deposition on southeast Alaskan glaciers (Figures 5 and 6). Based on a simple carbon isotopic mixing (Equation 1) of radiocarbon-dead and modern material ( $\Delta^{14}\text{C}$ :  $10$ – $105\text{‰}$ ), across these glacierized regions, a significant but variable fraction of DOC,  $12\%$ – $91\%$  (median  $50\%$ ), may be derived from fossil fuel combustion byproducts (Table 1). Together these data highlight regional variability in the role that fossil fuel combustion byproducts play in driving DOM composition in glacier ecosystems, demonstrating the importance of atmospherically deposited DOM and its source as a driver of glacier DOM composition and age.

The export of ancient glacier DOC is likely to have distinct ramifications for carbon cycling due to the liberation and incorporation of aged carbon in downstream food webs (Arimitsu et al., 2018; Fellman, Hood, Raymond, Hudson, et al., 2015; Hågvær & Ohlson, 2013; Hood et al., 2009). Our findings show that the ancient, likely fossil fuel-derived, component of DOC exists across a wide range of glacierized regions. This is direct evidence that anthropogenic deposition has impacted glacier carbon cycling on a global scale, and broadly acts as a carbon input to Earth's ecosystems, as proposed previously (e.g., Bauters et al., 2018; Budhavant et al., 2023; Fellman et al., 2015; Holt, Kellerman, et al., 2021, 2024; Li et al., 2016; Spencer, Guo, et al., 2014; Spencer, Vermilyea et al., 2014; Stubbins, Hood, et al., 2012; Xenopoulos et al., 2021). However, the extent that anthropogenic deposition drives glacier DOM composition clearly varies in space, and potentially in time. In relatively heavily fossil fuel impacted sites (e.g., in southeast Alaska), there is likely to be significant liberation of fossil fuel DOC. However, in glaciers like those studied here in Ecuador, the fossil fuel component of DOC is far smaller and glacier carbon cycling is predominantly driven by modern OC from the deposition of biomass burning-derived material and OM from in situ production. Glacier DOM is generally known to be highly biolabile compared to non-glacial watersheds underlain by contemporary soils, sup-

ported here by the high RA of aliphatic compounds in glacier outflows (Table 1; D'Andrilli et al., 2015; Hood et al., 2009). However, across these glacier outflows with  $^{14}\text{C-DOC}$  enrichment, there was an increased aliphatic content of DOM, which may increase the availability of biolabile compounds to aquatic microbial communities (D'Andrilli et al., 2015; Textor et al., 2019) and thus impact carbon cycling in receiving downstream or marine ecosystems. Since these changes in aliphatic content appear to have been in part linked to the origin of atmospherically deposited DOM, the source of atmospheric deposition to glacier surfaces, and generally Earth's ecosystems, may not only impact the age of carbon subsidy but also its lability and fate.

## Appendix A: Vanishing Glaciers Field Team

Patricio Andino<sup>8</sup>, Verónica Crespo-Pérez<sup>8</sup>, Moldobekov Bolt<sup>9</sup>, Ryskul Usabaliev<sup>9</sup>, Martina Schön<sup>7</sup>, Vincent De Staercke<sup>7</sup>, Michail Styllas<sup>7</sup> and Matteo Tolosano<sup>7</sup>. <sup>7</sup>River Ecosystems Laboratory, Ecole Polytechnique Fédérale de Lausanne, Lausanne, Switzerland. <sup>8</sup>Laboratorio de Limnología, Museo de Zoología QCAZ I, Escuela de

Ciencias Biológicas, Pontificia Universidad Católica del Ecuador, Quito, Ecuador. <sup>9</sup>Central-Asian Institute for Applied Geosciences, Bishkek, Kyrgyzstan.

## Global Research Statement

We thank Pontificia Universidad Católica del Ecuador and the Central-Asian Institute for Applied Geosciences for their support and use of resources during the field campaigns. We thank all the mountain refuges and guides for accommodating our work. Patricio Andino<sup>8</sup>, Verónica Crespo-Pérez<sup>8</sup>, Moldobekov Bolt<sup>9</sup>, Ryskul Usabaliev<sup>9</sup>, Martina Schön<sup>7</sup>, Vincent De Staercke<sup>7</sup>, Michail Styllas<sup>7</sup> and Matteo Tolosano<sup>7</sup> are thanked for their work as part of the Vanishing Glacier field team and for their support during field campaigns. All institutions that provided logistical field support can be found at <https://www.glacierstreams.ch/>.

## Data Availability Statement

Raw FT-ICR MS spectra files, calibrated peak list, and assigned elemental compositions are publicly available through the Open Science Framework (OSF; Holt et al., 2023).

## Acknowledgments

Dr. Anne M. Kellerman is thanked for help with sample preparation for FT-ICR MS. Amy Holt and Robert Spencer are extremely grateful to the Winchester Foundation and the International Association of Geochemistry for research support. A portion of this work was funded by the Vanishing Glaciers Project from the NOMIS Foundation to Tom Battin. Eran Hood and Jason Fellman were supported by National Science Foundation Alaska EPSCoR Program (OIA-1757348). 21 T FT-ICR MS analysis was performed in the Ion Cyclotron Resonance User Facility at the National High Magnetic Field Laboratory, which is supported by the National Science Foundation Division of Chemistry and Division of Materials Research through DMR 16-44779.

## References

- Andrews, M. G., Jacobson, A. D., Osburn, M. R., & Flynn, T. M. (2018). Dissolved carbon dynamics in meltwaters from the Russell Glacier, Greenland ice sheet. *Journal of Geophysical Research: Biogeosciences*, 123(9), 2922–2940. <https://doi.org/10.1029/2018jg004458>
- Antony, R., Grannas, A. M., Willoughby, A. S., Sleighter, R. L., Thamban, M., & Hatcher, P. G. (2014). Origin and sources of dissolved organic matter in snow on the East Antarctic ice sheet. *Environmental Science & Technology*, 48(11), 6151–6159. <https://doi.org/10.1021/es405246a>
- Antony, R., Willoughby, A. S., Grannas, A. M., Catanzano, V., Sleighter, R. L., Thamban, M., & Hatcher, P. G. (2018). Photo-biochemical transformation of dissolved organic matter on the surface of the coastal East Antarctic ice sheet. *Biogeochemistry*, 141(2), 229–247. <https://doi.org/10.1007/s10533-018-0516-0>
- Arimitsu, M. L., Hobson, K. A., Webber, D. A. N., Piatt, J. F., Hood, E. W., & Fellman, J. B. (2018). Tracing biogeochemical subsidies from Glacier runoff into Alaska's coastal marine food webs. *Global Change Biology*, 24(1), 387–398. <https://doi.org/10.1111/gcb.13875>
- Bauters, M., Drake, T. W., Verbeeck, H., Bodé, S., Hervé-Fernández, P., Zito, P., et al. (2018). High fire-derived nitrogen deposition on central African forests. *Proceedings of the National Academy of Sciences*, 115(3), 549–554. <https://doi.org/10.1073/pnas.1714597115>
- Bhatia, M. P., Das, S. B., Xu, L., Charette, M. A., Wadham, J. L., & Kujawinski, E. B. (2013). Organic carbon export from the Greenland ice sheet. *Geochimica et Cosmochimica Acta*, 109, 329–344. <https://doi.org/10.1016/j.gca.2013.02.006>
- Boix Canadell, M., Gómez-Gener, L., Ulseth, A. J., Cléménçon, M., Lane, S. N., & Battin, T. J. (2021). Regimes of primary production and their drivers in Alpine streams. *Freshwater Biology*, 66(8), 1449–1463. <https://doi.org/10.1111/fwb.13730>
- Bonilla, E., Mickley, L., Beaudon, E., Thompson, L., Rodriguez, W., Cruz Encarnación, R., et al. (2023). Contribution of biomass burning to black carbon deposition on Andean Glaciers: Consequences for radiative forcing. *Environmental Research Letters*, 18(2), 024031. <https://doi.org/10.1088/1748-9326/acb371>
- Budhavant, K., Andersson, A., Holmstrand, H., Satheesh, S., & Gustafsson, Ö. (2023). Black carbon aerosols over Indian Ocean have unique source fingerprint and optical characteristics during monsoon season. *Proceedings of the National Academy of Sciences*, 120(8), e2210005120. <https://doi.org/10.1073/pnas.2210005120>
- Cerling, T. E., Harris, J. M., MacFadden, B. J., Leakey, M. G., Quade, J., Eisenmann, V., & Ehleringer, J. R. (1997). Global vegetation change through the Miocene/Pliocene boundary. *Nature*, 389(6647), 153–158. <https://doi.org/10.1038/38229>
- Corilo, Y. (2014). *PetroOrg software*. Florida State University. All rights reserved.
- Csank, A. Z., Czimeczik, C. I., Xu, X., & Welker, J. M. (2019). Seasonal patterns of riverine carbon sources and export in NW Greenland. *Journal of Geophysical Research: Biogeosciences*, 124(4), 840–856. <https://doi.org/10.1029/2018jg004895>
- D'Andrilli, J., Cooper, W. T., Foreman, C. M., & Marshall, A. G. (2015). An ultrahigh-resolution mass spectrometry index to estimate natural organic matter lability. *Rapid Communications in Mass Spectrometry*, 29(24), 2385–2401. <https://doi.org/10.1002/rcm.7400>
- Ding, Y., Yamashita, Y., Jones, J., & Jaffé, R. (2015). Dissolved black carbon in boreal forest and glacial rivers of central Alaska: Assessment of biomass burning versus anthropogenic sources. *Biogeochemistry*, 123(1), 15–25. <https://doi.org/10.1007/s10533-014-0050-7>
- Dittmar, T., Koch, B., Hertkorn, N., & Kattner, G. (2008). A simple and efficient method for the Solid-Phase Extraction of Dissolved Organic Matter (SPE-DOM) from seawater. *Limnology and Oceanography: Methods*, 6(6), 230–235. <https://doi.org/10.4319/lom.2008.6.230>
- Fellman, J. B., Hood, E., Raymond, P. A., Hudson, J., Bozeman, M., & Arimitsu, M. (2015). Evidence for the assimilation of ancient Glacier organic carbon in a proglacial stream food web. *Limnology & Oceanography*, 60(4), 1118–1128. <https://doi.org/10.1002/lno.10088>
- Fellman, J. B., Hood, E., Raymond, P. A., Stubbins, A., & Spencer, R. G. M. (2015). Spatial variation in the origin of dissolved organic carbon in snow on the Juneau Icefield, Southeast Alaska. *Environmental science & technology*, 49(19), 11492–11499. <https://doi.org/10.1021/acs.est.5b02685>
- Feng, L., An, Y., Xu, J., Li, X., Jiang, B., & Liao, Y. (2020). Biochemical evolution of dissolved organic matter during snow metamorphism across the ablation season for a glacier on the central Tibetan plateau. *Scientific Reports*, 10(1), 1–10. <https://doi.org/10.1038/s41598-020-62851-w>
- Ginot, P., Schwikowski, M., Schotterer, U., Stüchler, W., Gäggeler, H. W., Francou, B., et al. (2002). Potential for climate variability reconstruction from Andean Glaciochemical records. *Annals of Glaciology*, 35, 443–450. <https://doi.org/10.3189/172756402781816618>
- Goránov, A. I., Schaller, M. F., Long, J. A. Jr., Podgorski, D. C., & Wagner, S. (2021). Characterization of Asphaltenes and Petroleum using Benzenepolycarboxylic Acids (BPCAs) and compound-specific stable carbon isotopes. *Energy & Fuels*, 35(22), 18135–18145. <https://doi.org/10.1021/acs.energyfuels.1c02374>
- Gul, C., Mahapatra, P. S., Kang, S., Singh, P. K., Wu, X., He, C., et al. (2021). Black carbon concentration in the central Himalayas: Impact on glacier melt and potential source contribution. *Environmental Pollution*, 275, 116544. <https://doi.org/10.1016/j.envpol.2021.116544>
- Häggvar, S., & Ohlson, M. (2013). Ancient carbon from a melting glacier gives high 14 C age in living pioneer invertebrates. *Scientific Reports*, 3(1), 1–4.

- Hendrickson, C. L., Quinn, J. P., Kaiser, N. K., Smith, D. F., Blakney, G. T., Chen, T., et al. (2015). 21 tesla Fourier transform ion cyclotron resonance mass spectrometer: A national resource for ultrahigh resolution mass analysis. *Journal of the American Society for Mass Spectrometry*, 26(9), 1626–1632. <https://doi.org/10.1007/s13361-015-1182-2>
- Holding, J. M., Duarte, C. M., Delgado-Huertas, A., Soetaert, K., Vonk, J. E., Agustí, S., et al. (2017). Autochthonous and allochthonous contributions of organic Carbon to microbial food webs in Svalbard fjords. *Limnology & Oceanography*, 62(3), 1307–1323. <https://doi.org/10.1002/lno.10526>
- Holt, A. D., Fellman, J., Hood, E., Kellerman, A. M., Raymond, P., Stubbins, A., et al. (2021). The evolution of stream dissolved organic matter composition following glacier retreat in coastal watersheds of Southeast Alaska. *Biogeochemistry*, 164, 1–18. <https://doi.org/10.1007/s10533-021-00815-6>
- Holt, A. D., Kellerman, A. M., Li, W., Stubbins, A., Wagner, S., McKenna, A., et al. (2021). Assessing the role of Photochemistry in driving the composition of dissolved organic matter in glacier runoff. *Journal of Geophysical Research: Biogeosciences*, 126(12), e2021JG006516. <https://doi.org/10.1029/2021jg006516>
- Holt, A. D., McKenna, A. M., Kellerman, A. M., Battin, T. I., Fellman, J. B., Hood, E., et al. (2024). Gradients of deposition and in situ production drive global glacier organic matter composition. *Global Biogeochemical Cycles*, 38(9), e2024GB008212. <https://doi.org/10.1029/2024gb008212>
- Holt, A. D., McKenna, A. M., & Spencer, R. (2023). P19289\_Glaciers provide insights into global black carbon deposition [Dataset]. *OSF*. <https://doi.org/10.17605/OSF.IO/U6MD8>
- Hood, E., Battin, T., Fellman, J., O'Neel, S., & Spencer, R. G. M. (2015). Storage and release of organic carbon from glaciers and ice sheets. *Nature Geoscience*, 8(2), 91–96. <https://doi.org/10.1038/ngeo2331>
- Hood, E., Fellman, J., Spencer, R. G. M., Hernes, P., Edwards, R., D'Amore, D., & Scott, D. (2009). Glaciers as a source of ancient and labile organic matter to the marine environment. *Letters to Nature*, 462(24), 1044–1048. <https://doi.org/10.1038/nature08580>
- Jaffé, R., Ding, Y., Niggemann, J., Vähätalo, A. V., Stubbins, A., Spencer, R. G. M., et al. (2013). Global charcoal mobilization from soils via dissolution and riverine transport to the oceans. *Science*, 340(6130), 345–347. <https://doi.org/10.1126/science.1231476>
- Kellerman, A. M., Vonk, J., McColough, S., Podgorski, D. C., van Winden, E., Hawkings, J. R., et al. (2021). Molecular signatures of glacial dissolved organic matter from Svalbard and Greenland. *Global Biogeochemical Cycles*, 35(3), e2020GB006709. <https://doi.org/10.1029/2020gb006709>
- Khan, A. L., Jaffé, R., Ding, Y., & McKnight, D. M. (2016). Dissolved black carbon in Antarctic lakes: Chemical signatures of past and present sources. *Geophysical Research Letters*, 43(11), 5750–5757. <https://doi.org/10.1002/2016gl068609>
- Khan, A. L., Wagner, S., Jaffé, R., Xian, P., Williams, M., Armstrong, R., & McKnight, D. (2017). Dissolved black carbon in the global cryosphere: Concentrations and chemical signatures. *Geophysical Research Letters*, 44(12), 6226–6234. <https://doi.org/10.1002/2017gl073485>
- Koch, B., & Dittmar, T. (2006). From mass to structure: An aromaticity index for high-resolution mass data of natural organic matter. *Rapid Communications in Mass Spectrometry*, 20(5), 926–932. <https://doi.org/10.1002/rcm.2386>
- Koch, B., & Dittmar, T. (2016). From mass to structure: An aromaticity index for high-resolution mass data of natural organic matter. *Rapid Communications in Mass Spectrometry*, 30(1), 250. <https://doi.org/10.1002/rcm.7433>
- Kohn, M. J. (2010). Carbon isotope compositions of terrestrial C3 plants as indicators of (Paleo) ecology and (Paleo) climate. *Proceedings of the National Academy of Sciences*, 107(46), 19691–19695. <https://doi.org/10.1073/pnas.1004933107>
- Lawson, E. C., Bhatia, M. P., Wadham, J. L., & Kujawinski, E. B. (2014). Continuous summer export of nitrogen-rich organic matter from the Greenland Ice Sheet inferred by ultrahigh resolution mass spectrometry. *Environmental science & technology*, 48(24), 14248–14257. <https://doi.org/10.1021/es501732h>
- Li, C., Bosch, C., Kang, S., Andersson, A., Chen, P., Zhang, Q., et al. (2016). Sources of black carbon to the Himalayan–Tibetan Plateau glaciers. *Nature Communications*, 7(1), 1–7. <https://doi.org/10.1038/ncomms12574>
- Li, C., Chen, P., Kang, S., Yan, F., Tripathi, L., Wu, G., et al. (2018). Fossil fuel combustion emission from South Asia influences precipitation dissolved organic carbon reaching the remote Tibetan Plateau: Isotopic and molecular evidence. *Journal of Geophysical Research: Atmospheres*, 123(11), 6248–6258. <https://doi.org/10.1029/2017jd028181>
- Magalhães, N. d., Evangelista, H., Condom, T., Rabatel, A., & Ginot, P. (2019). Amazonian biomass burning enhances tropical Andean glaciers melting. *Scientific Reports*, 9(1), 1–12.
- Musilova, M., Tranter, M., Wadham, J., Telling, J., Tedstone, A., & Anesio, A. M. (2017). Microbially driven export of labile organic carbon from the Greenland ice sheet. *Nature Geoscience*, 10(5), 360–365. <https://doi.org/10.1038/ngeo2920>
- Nagorski, S. A., Kaspari, S. D., Hood, E., Fellman, J. B., & Skiles, S. M. (2019). Radiative forcing by dust and black carbon on the Juneau Icefield, Alaska. *Journal of Geophysical Research: Atmospheres*, 124(7), 3943–3959. <https://doi.org/10.1029/2018jd029411>
- Rabatel, A., Francou, B., Soruco, A., Gomez, J., Cáceres, B., Ceballos, J. L., et al. (2013). Current state of glaciers in the tropical Andes: A multi-century perspective on glacier evolution and climate change. *The Cryosphere*, 7(1), 81–102. <https://doi.org/10.5194/tc-7-81-2013>
- Riedel, T., Biester, H., & Dittmar, T. (2012). Molecular fractionation of dissolved organic matter with metal salts. *Environmental science & technology*, 46(8), 4419–4426. <https://doi.org/10.1021/es203901u>
- Sato, M., Hansen, J., Koch, D., Lacis, A., Ruedy, R., Dubovik, O., et al. (2003). Global atmospheric black carbon inferred from AERONET. *Proceedings of the National Academy of Sciences*, 100(11), 6319–6324. <https://doi.org/10.1073/pnas.0731897100>
- Savory, J. J., Kaiser, N. K., McKenna, A. M., Xian, F., Blakney, G. T., Rodgers, R. P., et al. (2011). Parts-per-billion Fourier transform ion cyclotron resonance mass measurement accuracy with a “Walking” calibration equation. *Analytical Chemistry*, 83(5), 1732–1736. <https://doi.org/10.1021/ac102943z>
- Singer, G. A., Fasching, C., Wilhelm, L., Niggemann, J., Steier, P., Dittmar, T., & Battin, T. J. (2012). Biogeochemically diverse organic matter in Alpine glaciers and its downstream fate. *Nature Geoscience*, 5(10), 710–714. <https://doi.org/10.1038/ngeo1581>
- Smith, D. F., Podgorski, D. C., Rodgers, R. P., Blakney, G. T., & Hendrickson, C. L. (2018). 21 tesla FT-ICR mass spectrometer for ultrahigh-resolution analysis of complex organic mixtures. *Analytical Chemistry*, 90(3), 2041–2047. <https://doi.org/10.1021/acs.analchem.7b04159>
- Spencer, R. G. M., Guo, W., Raymond, P. A., Dittmar, T., Hood, E., Fellman, J., & Stubbins, A. (2014). Source and biolability of ancient dissolved organic matter in glacier and lake ecosystems on the Tibetan Plateau. *Geochimica et Cosmochimica Acta*, 142, 64–74. <https://doi.org/10.1016/j.gca.2014.08.006>
- Spencer, R. G. M., Stubbins, A., Hernes, P. J., Baker, A., Mopper, K., Aufdenkampe, A. K., et al. (2009). Photochemical degradation of dissolved organic matter and dissolved lignin phenols from the Congo River. *Journal of Geophysical Research*, 114(G3). <https://doi.org/10.1029/2009jg000968>
- Spencer, R. G. M., Vermilyea, A., Fellman, J., Raymond, P., Stubbins, A., Scott, D., & Hood, E. (2014). Seasonal variability of organic matter composition in an Alaskan glacier outflow: Insights into glacier carbon sources. *Environmental Research Letters*, 9(5), 55005. <https://doi.org/10.1088/1748-9326/9/5/055005>



- Stubbins, A., & Dittmar, T. (2012). Low volume quantification of dissolved organic carbon and dissolved nitrogen. *Limnology and Oceanography: Methods*, 10(5), 347–352. <https://doi.org/10.4319/lom.2012.10.347>
- Stubbins, A., Hood, E., Raymond, P. A., Aiken, G. R., Sleighter, R. L., Hernes, P. J., et al. (2012). Anthropogenic aerosols as a source of ancient dissolved organic matter in glaciers. *Nature Geoscience*, 5(3), 198–201. <https://doi.org/10.1038/ngeo1403>
- Stubbins, A., Niggemann, J., Dittmar, T., & Herndl, G. (2012). Photo-lability of deep ocean dissolved black carbon. *Biogeosciences*, 9(5), 1661–1670. <https://doi.org/10.5194/bg-9-1661-2012>
- Stubbins, A., Spencer, R. G. M., Mann, P. J., Holmes, R. M., McClelland, J. W., Niggemann, J., & Dittmar, T. (2015). Utilizing colored dissolved organic matter to derive dissolved black carbon export by arctic rivers. *Frontiers in Earth Science*, 3, 63. <https://doi.org/10.3389/feart.2015.00063>
- Textor, S. R., Wickland, K. P., Podgorski, D. C., Johnston, S. E., & Spencer, R. G. (2019). Dissolved organic carbon turnover in permafrost-influenced watersheds of interior Alaska: Molecular insights and the priming effect. *Frontiers in Earth Science*, 7, 275. <https://doi.org/10.3389/feart.2019.00275>
- Tranter, M. (2012). Ancient organics reign on glaciers. *Nature Geoscience*, 5(3), 167–168. <https://doi.org/10.1038/ngeo1411>
- Vaezzadeh, V., Yi, X., Thomes, M. W., Bong, C. W., Lee, C. W., Zakaria, M. P., et al. (2021). Use of molecular markers and compound-specific isotopic signatures to trace sources of black carbon in surface sediments of Peninsular Malaysia: Impacts of anthropogenic activities. *Marine Chemistry*, 237, 104032. <https://doi.org/10.1016/j.marchem.2021.104032>
- Wagner, S., Brandes, J., Goranov, A. I., Drake, T. W., Spencer, R. G. M., & Stubbins, A. (2017). Online quantification and compound-specific stable isotopic analysis of black carbon in environmental matrices via liquid chromatography-isotope ratio mass spectrometry. *Limnology and Oceanography: Methods*, 15(12), 995–1006. <https://doi.org/10.1002/lom3.10219>
- Wagner, S., Brandes, J., Spencer, R. G. M., Ma, K., Rosengard, S. Z., Moura, J. M. S., & Stubbins, A. (2019). Isotopic composition of oceanic dissolved black carbon reveals non-riverine source. *Nature Communications*, 10(1), 1–8. <https://doi.org/10.1038/s41467-019-13111-7>
- Wagner, S., Jaffé, R., & Stubbins, A. (2018). Dissolved black carbon in aquatic ecosystems. *Limnology and Oceanography Letters*, 3(3), 168–185. <https://doi.org/10.1002/lol2.10076>
- Xenopoulos, M. A., Barnes, R. T., Boodoo, K. S., Butman, D., Catalán, N., D'Amario, S. C., et al. (2021). How humans alter dissolved organic matter composition in freshwater: Relevance for the Earth's biogeochemistry. *Biogeochemistry*, 154(2), 1–26. <https://doi.org/10.1007/s10533-021-00753-3>
- Xian, F., Hendrickson, C. L., Blakney, G. T., Beu, S. C., & Marshall, A. G. (2010). Automated broadband phase correction of Fourier transform ion cyclotron resonance mass spectra. *Analytical Chemistry*, 82(21), 8807–8812. <https://doi.org/10.1021/ac101091w>
- Xu, L., Roberts, M. L., Elder, K. L., Kurz, M. D., McNichol, A. P., Reddy, C. M., et al. (2021). Radiocarbon in dissolved organic carbon by Uv oxidation: Procedures and blank Characterization at Nosams. *Radiocarbon*, 63(1), 357–374. <https://doi.org/10.1017/rdc.2020.102>
- Yarnes, C., Santos, F., Singh, N., Abiven, S., Schmidt, M. W., & Bird, J. A. (2011). Stable isotopic analysis of pyrogenic organic matter in soils by liquid chromatography–isotope-ratio mass spectrometry of benzene polycarboxylic acids. *Rapid Communications in Mass Spectrometry*, 25(24), 3723–3731. <https://doi.org/10.1002/rcm.5272>
- Yu, H., Remer, L. A., Chin, M., Bian, H., Tan, Q., Yuan, T., & Zhang, Y. (2012). Aerosols from overseas rival domestic emissions over North America. *Science*, 337(6094), 566–569. <https://doi.org/10.1126/science.1217576>

## References From the Supporting Information

- Behnke, M. I., Stubbins, A., Fellman, J. B., Hood, E., Dittmar, T., & Spencer, R. G. (2020). Dissolved organic matter sources in Glacierized watersheds delineated through compositional and carbon isotopic modeling. *Limnology & Oceanography*, 66(2), 438–451. <https://doi.org/10.1002/lno.11615>
- Fischer, M., Huss, M., Barboux, C., & Hoelzle, M. (2014). The new Swiss Glacier Inventory SGI2010: Relevance of using high-resolution source data in areas dominated by very small glaciers. *Arctic Antarctic and Alpine Research*, 46(4), 933–945. <https://doi.org/10.1657/1938-4246-46.4.933>
- Kohler, T. J., Bourquin, M., Peter, H., Yvon-Durocher, G., Sinsabaugh, R. L., Deluigi, N., et al. (2024). Global emergent responses of stream microbial metabolism to glacier shrinkage. *Nature Geoscience*, 17(4), 309–315. <https://doi.org/10.1038/s41561-024-01393-6>
- Young, J. C., Pettit, E., Arendt, A., Hood, E., Liston, G. E., & Beamer, J. (2021). A changing hydrological regime: Trends in magnitude and timing of glacier ice melt and glacier runoff in a high latitude coastal watershed. *Water Resources Research*, 57(7), e2020WR027404. <https://doi.org/10.1029/2020wr027404>